A rapid and quantitative safranin-based fluorescent microscopy method to evaluate cell wall lignification

Fabien Baldacci-cresp, Corentin Spriet, Laure Twyffels, Anne-Sophie Blervacq, Godfrey G. Neutelings, Marie Baucher, Simon Hawkins

the plant journal

A rapid and quantitative safranin-based fluorescent microscopy method to evaluate cell wall lignification

Journal:	*The Plant Journal*
Manuscript ID	Draft
Manuscript Type:	Technical Advance
Biochemistry and Physiology:	
Cell Biology:	Cell wall
Genomics & Genetics:	
Plant Growth & Development:	
Plant interactions with other organisms:	
Plant Responses to Environment:	
Other (please specify):	

A rapid and quantitative safranin-based fluorescent microscopy method to evaluate cell wall lignification

Fabien Baldacci-Cresp[1,2], Corentin Spriet[1,3], Laure Twyffels[4], Anne-Sophie Blervacq[1], Godfrey Neutelings[1], Marie Baucher[2] and Simon Hawkins[1].

[1] Université de Lille, CNRS, UMR 8576 – UGSF - Unité de Glycobiologie Structurale et Fonctionnelle, F-59000 Lille, France.

[2] Université libre de Bruxelles, Laboratoire de Biotechnologie Végétale (LBV), B-6041 Gosselies, Belgium.

[3] TISBio, Université de Lille, CNRS, UMR 8576 – UGSF - Unité de Glycobiologie Structurale et Fonctionnelle, F-59000 Lille, France.

[4] Université libre de Bruxelles, Center for Microscopy and Molecular Imaging (CMMI), B-6041 Gosselies, Belgium.

Corresponding Author: Fabien Baldacci-Cresp & Simon Hawkins

fabien.baldacci-cresp@univ-lille.fr & simon.hawkins@univ-lille.fr

E-mail addresses: Fabien Baldacci-Cresp: fabien.baldacci-cresp@univ-lille.fr; Corentin Spriet : cspriet@univ-lille.fr; Laure Twyffels : Laure.Twyffels@ulb.ac.be; Anne-Sophie Blervacq : anne-sophie.blervacq@univ-lille.fr; Godfrey Neutelings : godfrey.neutelings@univ-lille.fr; Marie Baucher: mbaucher@ulb.ac.be; Simon Hawkins : simon.hawkins@univ-lille.fr

SUMMARY

One of the main characteristics of plant cells is the presence of the cell wall located outside the plasma membrane. In particular cells, this wall can be reinforced by lignin, a polyphenolic polymer that plays a central role for vascular plants, conferring hydrophobicity to conducting tissues and mechanical support for upright growth. Lignin has been extensively studied by a range of different techniques including anatomical and morphological analyses using dyes to characterize the polymer localization *in situ*. With the constant improvement of imaging techniques, it is now possible to revisit old qualitative techniques and adapt them to obtain efficient, highly resolutive, quantitative, fast and safe methodologies. In this study, we revisit and exploit the potential of fluorescent microscopy coupled to safranin-O staining to develop a quantitative approach for lignin content determination. The developed approach is based on ratiometric emission measurements and the development of an ImageJ macro. To demonstrate the interest of our methodology compared to other commonly-used lignin reagents, we showed that safranine-O staining was used to evaluate and compare lignin contents in previously characterized *A. thaliana* lignin biosynthesis mutants. In addition, the analysis of lignin content and spatial distribution in the Arabidopsis laccase mutant also provided new biological insights into the effects of *laccase* gene down-regulation in different cell types. Our safranine-O based methodology, also validated for flax, maize and poplar, significantly improves and speed-up anatomical and developmental investigations of lignin, which we hope will contribute to new discoveries in many areas of cell wall plant research.

SIGNIFICANCE STATEMENT (2 sentences 75 words max)

Lignin has long been the subject of extensive study as it plays a major role in plant growth and defense and is an important factor affecting the quality of plant biomass and plant-derived products. The development of an easy and quantitative confocal microscopy method to provide detailed spatial information about lignin content at the cell wall level will prove a valuable addition to the toolbox of lignin analytical methods for both fundamental and applied research.

INTRODUCTION

A main characteristic of the plant cell is the presence of a cell wall. This wall allows plant cells to acquire a certain rigidity essential for the maintenance of a strong intracellular osmotic pressure that contributes to maintaining the plant stem upright. Depending upon cell types, this wall can be mainly composed of up to three layers. The first one is the middle lamella, a thin structure mainly composed of pectins and shared by two adjacent cells. This layer is the pedestal on which the two other structures – the primary and the secondary cell walls - can be developed. The primary wall is the first to be deposited and is mainly composed of cellulose, hemicelluloses, pectins and proteins (Carpita and Gibeaut, 1993). In certain tissues, plant cells acquire a secondary wall that is deposited between the primary cell wall and the plasma membrane. Like primary cell walls, secondary cell walls are rich in cellulose, but generally show higher hemicellulose and lower pectin content providing greater mechanical strength and reduced extensibility. This secondary cell wall, generally much thicker than the primary wall and made of several layers (S1, S2 and S3), is mainly observed in cells from vascular and supporting tissues. The formation of the secondary cell wall is, in most cases, associated with the deposition of lignin that confers hydrophobicity and rigidity to the cell wall (Boerjan et al., 2003). Lignin is a phenolic polymer composed of 3 main units, *p*-hydroxyphenyl (H), guaiacyl (G) and syringyl (S) units derived fom *p*-coumaryl alcohol, coniferyl alcohol and sinapyl alcohol, respectively. The biosynthesis of lignins is initiated during the formation of the S1 secondary cell wall layer and newly formed lignin is first observed in the cell corners and middle lamella before spreading progressively, to the primary cell wall and different layers (S1, S2 and S3) of the secondary cell wall (Terashima and Fukushima, 1988). Given the major importance of lignin – both for the plant and economically - it is not surprising that the biosynthesis/polymerization and degradation of this polymer have been extensively studied for a very long time (Boerjan et al., 2003).

One of the major challenges of recent and future years is to improve our ability to characterize, both quantitatively and qualitatively, lignin in plant cell walls. In terms of quantitative analysis, three main types of wet chemistry methods are traditionally used: acetylbromide assays (Morrison, 1972b, Morrison, 1972a), the acidic method (Van Soest, 1963) or the Klason method (Johnson et al., 1961). If

the Klason method seems more suitable and efficient on woody species, the acetylbromide and the acidic methods are more suitable for herbaceous species. In these species, the acetyl bromide method is faster and presents a better recovery of lignin (Fukushima et al., 2015).

Various types of methods are also available for determining lignin chemical composition (i.e. determination of S, G and H contents and calculation of S/G ratios). There include chemical degradation techniques, such as thioacidolysis (Lapierre et al., 1986) and nitrobenzene oxidation (Monties, 1989), as well as derivatization methods and spectroscopic methods based on NMR (Mansfield et al., 2012) or using pyrolysis-GC/MS coupling (Wagner et al., 2007).

If these qualitative and quantitative approaches are powerful, they all present the same drawback: they are destructive methods that require grinding and/or extraction of cell wall polymers/lignins from the plant sample being analyzed. As a result, the data obtained represent an overall mean value for a whole organ/tissue and thus do not take into account the fact that lignin content and composition vary between different tissues, cells and cell wall layers. To get around this problem and to obtain information on lignin localization more rapidly, researchers have exploited different histochemical methods including basic fushin and auramine staining (epifluorescence observations) (Dharmawardhana et al., 1992, Pesquet et al., 2005) revealing global lignin deposition, as well as more 'specific' tests such as phloroglucinol staining (Weisner reagent) revealing lignin hydroxycinnamaldehyde functions (Vallet et al., 1996, Liljegren, 2010), and Maüle staining providing indications on the S/G ratio (Meshitsuka and Nakano, 1979). Another approach based on safranin/alcian blue staining, the FASGA method (Tolivia and Tolivia, 1987), coupled to an adapted image workflow (Legland et al., 2017) allows a quantification of the histology of maize based on lignin-containing tissues detection but does not permit a strict quantification of cell wall lignin content.

Other approaches based on micro-vibrational spectroscopy (IR and Raman) were successfully adapted to plant biology and more particularly to *in situ* cell wall characterization (Gierlinger, 2014, Agarwal, 2006, Agarwal and Ralph, 1997, Gierlinger, 2018). They allow scientists to obtain qualitative, quantitative and spatial data on lignin. However, microspectroscopy approaches are generally very difficult to calibrate in terms of acquisition analysis and are also time consuming for both machine use

and data analyses. Overall, such methodology is not adapted for the rapid measurement of lignin content in a tissue/sample compared to a reference and can therefore represent an inconvenience for functional genomics approaches that can involve the analyses of large numbers of samples (e.g. mutant populations, biological replicates).

In 2008, Bond and co-authors (Bond et al., 2008) demonstrated that the azo dye safranin-O, commonly used with a counterstain to color lignified cell walls red in botanical samples examined by transmitted light in the visible spectrum, also presents an interesting fluorescence characteristic. Using a range of different plant samples made up of cells with high or low lignin levels these authors showed that the safranin-O emission spectrum depends on lignin quantity – the higher the lignin content of the stained tissue, the more intense the red part of the emission spectrum. While providing a novel way to distinguish lignin-rich from cellulose-rich cell walls without the need for counterstaining, their approach remained qualitative and did not allow for statistical comparison of lignin levels in different samples, We therefore decided to develop a technique that would i) generate high definition spatial information about lignin localization, ii) provide quantitative information that can be analyzed to support statistically significant differences in lignin content between samples, and iii) be fast, easy and low-risk for the experimenter.

RESULTS

Safranin emission spectra depends on lignin content

Bond and co-authors (Bond et al., 2008) demonstrated that the safranin emission spectrum changes according to cell wall lignin content. Higher lignin amount induces a relative increase in the red part of the emission spectrum. This effect can be clearly seen in the safranin-O spectra (under 488 nm excitation) obtained from different cell walls (zones 1-4) in a stem cross-section from a 2-month-old flax plant (Fig. 1). We used flax as an appropriate model plant to develop the safranin-based methodology since the stem of this species contains two populations of cells with highly contrasted secondary cell wall lignification profiles: xylem cells with a highly lignified secondary walls and cortical bast fibers with poorly lignified secondary cell walls (Day et al., 2005). This allowed us to observe different levels of cell wall lignification within the same histological section as shown with the toluidine blue staining in Fig. 1a.

Analysis of the Safranin fluorescence emission spectra under 488 nm excitation of different flax stem cell types (Fig. 1b) indicated that the maximum peak intensity is 570 nm regardless of cell type analyzed. Spectral analysis shows that the more lignified the cell wall is, the higher the emission spectrum in the orange and red region (570 - 600 nm) (Fig. 1b). In contrast, the "green" part of the spectrum (520 - 560 nm) remains stable indicating that it is the orange/red part of the spectrum that discriminates between the different cell walls analyzed. Beyond 600 nm, the variability is lost.

Based on these observations, we decided to develop a ratiometric emission spectrum approach for evaluating cell wall lignification levels that would be robust, both within a histological section and between histological sections from different provenances (e.g. species, genotype, age).

Method development: from sample preparation to image treatment.

We firstly developed a standardized methodology designed to limit time consumption and risk to the manipulator without altering result quality (Method S1 and Fig. S1). The aim of the first (facultative) step with EtOH alcohol is to fix and conserve samples (up to several weeks in 70 % EtOH) for later analysis as well as to limit the autofluorescence of pigments (e.g. chlorophyll) that can interfere with

safranin fluorescent emission. The time necessary for this step must be defined depending upon the considered sample but an overnight incubation is usually suitable for most samples. As described later, it is important to have flat cross-sections and, in this case, samples are sectioned with a vibroslicer as thinely as possible (30-100µm) to obtain the best morphology. However, since the methodology is based on epifluorescence the thickness of the cut will not unduly influence image acquisition. Next, a 10 min staining step in safranin-O alcoholic solution (0.2 % in 50 % EtOH) is performed at room temperature in the dark with shaking. This step is followed by a short rinse with 50% EtOH to remove safranin excess on the tube/plate, a 15 min rinse with 50% EtOH and 2 x 10 min H_2O rinses under shaking in the dark to remove excess safranin. Samples are subsequently mounted in distilled water and analyzed with a confocal microscope.

Before starting any comparative confocal analyses, it is important to obtain safranin spectra of lignified and non-lignified cell walls from the plant sample so as to determine invariable “green” channel and variable “red” channel values. Then, for each series of observations on a given sample, it is necessary to calibrate laser intensity and time acquisition. The more these two values are low, the less there will be a risk of safranin spectra shift as discussed later. Since our methodology is based on fluorescence quantification, the chosen laser intensity and time acquisition must provide enough fluorescence intensity per pixel whilst avoiding saturation. Finally, it is mandatory to select a flat area of the sample for observation.

Spectrum acquisition provides images of the type presented in Fig. 2a, b and c. The corresponding image file is then treated with the developed ImageJ macro. This macro applies a region of interest (ROI) selection, a noise threshold subtraction, a 32-bit conversion and a median radius filter. Next, it defines the highest intensity value, applies a threshold and converts the background to NaN. At this moment there are two possibilities for the user: leave the automatic threshold selection, or manually correct this threshold so as to make it more coherent with your knowledge of your sample morphology. Finally, the ratio calculation is made and a ratiometric image is generated as presented in Fig 2c.

Default settings allow the user to obtain an image representation on a color scale from purple to red in a ratio range from 0 (purple) to 2 (red). In our context, black pixels correspond to NaN pixels without

ratiometric value (under the threshold, not considered in measurement even if selected). Purple pixels correspond to pixels with ratiometric value close to 0. In the case where the default range does not lead to useful image representation, it can be restricted or enlarged (Fig. S2). It is important to be careful at this stage since a valid comparison of different images requires that they are all built using the same range.

In addition to the ratiometric image, the macro also allows a quantitative representation. For this, the user selects the ROI on the ratiometric image and makes a measurement with image J (Fig. 2d). The same method is then applied to further ROIs allowing statistical analysis.

Biological validation of the method in Arabidopsis

In order to test the robustness of our technique and its capacity to generate biologically relevant information on cell wall lignin content we applied it to different model plant species. We first evaluated the ratiometric technique in different lignin mutants from *Arabidopsis thaliana*. The lignin biosynthetic pathway has been extensively studied in this species over the last 20 years and modifications in lignin content/structure have been well characterized in a number of different mutants making them ideal test objects for our technique. Our results (Fig. 3) show that the ratiometric values of fiber cell walls in *cinnamyl alcohol dehydrogenase* (*CAD*) and *caffeic acid* O-*methyl transferase* (*COMT*) (Fig. 3b, e) mutants are not significantly different from those of WT plants (Fig. 3a, d). While both mutants contain similar amounts of lignin to WT plants, *cad* mutants possess lignin with a higher aldehyde content and *comt* mutants show an altered S/G lignin monomer ratio (Van Acker et al., 2013). The fact that the ratiometric values remain unchanged suggests that our safranin ratiometric technique is insensitive to differences in lignin structures. In contrast, similar analyses on the *f5h* mutant (Fig. 3c) revealed a significant increase in the red/green ratiometric value indicating higher lignin content (9 %) in agreement with previous lignin chemical analyses (Van Acker et al., 2013). Taken together, these results indicate that the safranin ratiometric technique reflects cell wall lignin content but is not affected by lignin composition making it a powerful *in situ* analytical method for lignin quantitative analysis.

As another example we investigated the *lac4-2 lac17* double mutant previously characterized by Berthet and co-authors (Berthet et al., 2011). Destructive wet chemistry analysis (acetyl bromide) indicated that this mutant contains 40 % less lignin in floral stems as compared to WT plants and shows weaker staining of interfascicular fibers with the Weisner reagent. The application of our technique to floral stem cross-sections from this mutant enabled us to both confirm previous observations and obtain more detailed information about the effect of the mutation on the cell wall phenotype (Fig. 4). Firstly, mutant interfascicular fiber cell walls are thickened, but have less well-organized inner secondary cell walls in comparison with WT sections (Fig. 4a and b). Secondly, lignification appears to be restricted to the middle lamella and primary cell wall of mutants compared to WT fibers that also possess lignified secondary cell walls. In addition to these observations that confirm the results obtained by Berthet et al., our method also allowed us to obtain quantification on the amount of lignin reduction in fiber cell walls. Examination of average ratiometric values (Fig. 4c) indicated that mutant fiber lignin content was reduced by about 50 % compared to WT cell walls. These values are higher than the reduction in Klason lignin values (30 – 40 %) determined by Berthet and co-workers but were obtained from analysis of the whole stem that contains both interfascicular fibers and fiber bundles.

The differences between the values obtained by safranin and wet chemistry of whole stems could suggest that the reduction in cell wall lignin is higher in fibers compared to vascular bundles and we therefore decided to analyze cell walls in the latter region. The analysis of cell walls in vascular bundles (Fig. 4d - f) show that there is no significant difference in mean cell wall lignin levels between WT and mutant plants when overall mean values for the bundle are taken into account. This result suggests that the 30-40 % reduction in Klason lignin values reported by Berthet and coworkers is due to a proportionally greater reduction in fibers compared to vascular bundles and indicates that the *lac4-2 lac17* double mutation affects the lignification process in different ways depending upon the tissue considered.

The safranin ratiometric approach also allowed us to obtain new information about the effect of the mutation at the cell/cell wall layer level. For example, when the maximum (and not the mean) ratio values obtained from the lignified zones of WT fibers (middle lamella, primary cell wall, secondary cell wall) and mutant fibers (middle lamella, primary cell wall) are considered (Fig. 4c) the values indicate

that lignin levels in middle lamella and primary cell walls are comparable. Taken together these results indicate that the *lac4-2 lac17* mutation primarily affects secondary cell wall lignification (but not middle lamella/primary cell wall lignification) and is associated with increased secondary cell wall thickness - potentially in an attempt to compensate the loss of rigidity due to reduced lignification. The ratiometric approach also generates intriguing information about the effect of the mutation on the lignification process in vessels. Indeed, our results would suggest that the down-regulation of the *Lac4* and *Lac17* genes is not associated with a decrease in overall vascular bundle lignin content, but is, in fact, associated with increased lignification in xylem vessel cell walls and decreased lignification in fiber cell walls within the vascular bundle. Interestingly, mutant vascular bundles appear to contain a higher proportion of xylem fibers with poorly-lignified walls thereby underlining the existence of cell specific lignification programs.

In conclusion, the use of our safranin-based imaging approach allowed us to obtain both quantitative and precise spatial information about cell wall lignin content in a single experiment and on the same sample thereby providing a considerable advantage over chemical analysis (quantitative data, but loss of spatial information) or other histochemical reagents such as Weisner (spatial information, but no quantitative data).

Biological validation of the method in other plant species

The applicability of our method was used to investigate cell wall lignin in the flax *lbf1* mutant that is characterized by the presence of bast fibers with a secondary cell wall lignin content of around 17 % compared to 5 % in WT plants (Chantreau et al., 2014). These values were obtained by destructive wet chemistry (acetyl bromide) and mask a strong spatial heterogeneity. As shown in Figure 5, the safranin ratio of bast fibers varies from 0 to 7 unit (safranin ratio mean of 1.2 unit corresponding to 2.4 times more lignin signal than WT) in a first developmental stage of lignification in 4-week-old plants (Fig. 6b and d) and from 0 to 15 (safranin ratio mean of 2.2; 4.4 times more lignin signal than WT) in a more advanced developmental stage of lignification (fig. 5c and d).

Lignin content was also evaluated in the cell walls of maize, a monocotyledon plant. On stem cross sections various tissues with different lignin levels were observed with a 4x objective (Fig. 6a). Non-lignified parenchyma cell walls appear in black i.e. under the detection threshold of our methodology. Hypodermis cell walls are colored in blue indicating low lignin levels (safranin ratio = 0.53) in comparison with the more heavily lignified cell walls of the epidermis (safranin ratio =0.93) and vascular bundle sheath that appear red (safranin ratio = 0.98) (Fig. 6a). This approach is complementary to an approach based on the bioinformatic treatment of FASGA stained stem sections that allows genotyping based on the surface of lignification (Legland et al., 2017). The safranin ratio methodology also allows a better resolution as it is independent of the section thickness that can become a limiting point when the cell density and therefore the opacity to the transmitted light are too important, as it occurs in the vicinity of large metaxylem vessels (Figure 6b). Sclerenchyma cell walls (red) are more lignified than vessels (blue to yellow) or phloem cell walls (purple, blue) (Figure 6b). Also, the development and the associated lignification appears polarized with 5 to 6 lignified cell layers on the protoxylem side against 1 to 3 cell layers on the phloem side. Altogether, these results confirm that the safranin approach can be easily applied to both monocots and dicots and provides highly detailed ratiometric quantitative data on cell wall lignin levels in comparison with global wet chemistry analyses which are longer and more laborious to set up.

The finesse of analyzes beyond simple quantification.

The described safranin method is not only easy to use, but also provides a high resolution spatial information on cell wall lignin that can usually only be obtained by using more time-consuming and fastidious techniques such as light/SEM immunolocalisation or Raman spectroscopy (Gierlinger, 2018, Kiyoto et al., 2013, Day et al., 2005, Simon et al., 2018).

An example of high-resolution using the safranin technique is illustrated in Figure 7 showing the results of an analysis of flax stem xylem. In contrast to other classical histological analyzes (eg. phloroglucinol-HCl) that suggest a uniform lignification of xylem cell walls (Day et al. 2005; Huis et al., 2012), our methodology indicates that periclinal cell walls often contain higher amounts of lignin than anticlinal cell walls (Fig. 7a). Similarly, examination of a pit between two fiber tracheids at 60x magnification

(Fig. 7b) provides an image quality and detailed information that approaches that obtained by electron microscopy (Fromm et al., 2003). The obtained image reveals the localized high lignin levels in the vicinity of the pit as well as in the compound middle lamella between the two cells.

Technical controls – limits to be respected.

As in most imaging approaches, it is important to control different technical aspects that can affect the acquired signal and may lead to the generation of artifacts and false interpretations.

A first parameter is related to sample thickness and the focal plane at which observations are made. The lower the focal plane (i.e. the deeper within the section that one goes), the more incident laser energy and the resulting emission energy will be decreased. The extent to which this occurs is likely to be different depending upon the wavelength considered. To characterize this phenomenon in our methodology, we analyzed green and red channel fluorescence intensities of fiber cell walls at different focal planes in a section of safranin-O stained poplar xylem (Fig. 8). Our results show that the fluorescence intensity of the two channels is identical for the first 9 optical sections (upper to lower) and increases from around 70% of maximum intensity in the first optical section to 100% at the 9th optical section. From the tenth optical section onwards, signal intensity decreases for the 2 channels but to a greater extent for the green channel compared to the red channel. These results indicate that the good benchmark for undertaking analysis is when the sample appears focused in the green channel.

An additional requirement resulting from this phenomenon is that the sample prepared is flat. As shown in the Figure 8, an uneven sample when analyzed at a given z-depth will give a different result depending upon the tissue thickness crossed. In Figure 8b, at the surface of the sample section, only the xylem appears in blue (Fig. 8b, i) whereas deeper in the section, other tissues appear first in blue and then in yellow and the initial xylem which appears in yellow and then redder (Fig 8b, ii to iv).

A second parameter concerns the fluorophore's resistance to bleaching. Since the technique depends on a ratiometric approach, the absolute intensity level does not matter, and it is more important to check the ratiometric stability. To evaluate this parameter, we subjected images of a 3-month-old poplar stem cortical fiber stained by safranin-O to increasing (intensity and accumulation time per pixel) excitation

(Fig. 9). For this, we exposed the sample at a laser intensity of 5% (Fig. 9a-c) and 100% (Figure 9d-f) on continuous acquisition (20s / acquisition - 512x512 pixels image). At 5% laser intensity (Fig. 9a-c), differences in the percentage red/green ratio between the first and the fifteenth passage were of the order of 4%, whereas this value increased to around 35 % when 100% laser intensity was used (Figure 9d-f, g) resulting in a very different visual image depending upon total (intensity and time) laser energy used (Fig. 9h). Such a result indicates that excessive excitation of safranin affects its spectral properties and provokes a photoinduced spectral shift in favor of green wavelengths. Analyses should therefore be performed at low (power and/or time) excitation levels in order to keep any potential changes in the red/green ratio to a minimum.

DISCUSSION

Lignin is the third most abundant biopolymer on Earth and plays a vital role in many aspects of plant life (1). The presence and structure of this polymer also have an important impact on the quality of a wide range of different plant-based resources and is therefore of major economic importance. Together with other cell wall polymers, lignin also represents a major sink for atmospheric carbon and its biosynthesis therefore contributes to counteracting climate change (Bastin et al., 2019). It is therefore not surprising that scientists have developed a wide range of different techniques for studying this important polymer.

Many different chemical and physical techniques are available to quantify and structurally characterize lignin in plant cell walls (Simon et al., 2018) and have been successfully used on both highly lignified tissues from woody plants and on more weakly lignified samples such as those found in herbaceous species.

However, many of these dosage methods are destructive and do not take into account the variability in lignin quantity and structure that occurs between different cell types and/or cell wall layers. As a result, the potential role of genes in the regulation of lignin biosynthesis and deposition at the cellular level is often ignored or simplified. This aspect is particularly important given recent reports demonstrating that

the deposition of lignin in the cell wall is either under the spatial control of particular proteins localized in the cell wall (Yi Chou et al., 2018, Hosmani et al., 2013, Tobimatsu and Schuetz, 2019).

In contrast to destructive quantitative techniques, a number of *in situ* non-destructive techniques including classic light microscopy histochemistry, UV microscopy, TEM immunolocalisation and Raman spectroscopy can also be used to analyse cell wall lignin (Simon et al., 2018).

Of these, it is perhaps the Maüle and Wiesner staining methods that are the most widely used light microscope approaches for analysing lignin *in situ* (Monties, 1989). The Wiesner reagent (phloroglucinol-HCl) colours lignified cell walls in red and the Maüle reaction brings information about the S/G ratio. Both of these methods are relatively rapid, easy to use and accessible to most labs that possess a standard light microscope. However, they do not provide quantitative data thereby preventing statistical comparisons of cell wall lignin levels, either within the same sample, or between different samples. In addition, care should also be taken with the Wiesner reagent as it only highlights the aldehyde groups present in the polymer. In this paper we developed a simple and rapid confocal fluorescence imaging approach based on safranin-O histochemistry and that is able to provide both detailed spatial information and quantitative data on cell wall lignin levels.

Safranin-O is a basic azo dye that binds to the acidic lignin polymer (it is believed to form pi-pi interactions with the polymer (Stockert et al., 1984). Using a range of plant samples characterized by the presence of cells showing different amounts of cell wall lignin, Bond and co-workers demonstrated that cell walls/cell wall regions containing high lignin levels (e.g. cell corners of pine wood) exhibited red fluorescence in safranin-O-stained samples observed by confocal microscopy, while non-lignified cell walls (cotton fibers, poplar wood G-layers) fluoresced green. This same study also demonstrated that the red fluorescence in safranin-O stained samples was spatially correlated with high lignin autofluorescence in non-stained samples confirming the correlation between lignin quantity and red fluorescence.

Since a number of different factors can affect the intensity of acquired signals, we firstly undertook a number of experiments to standardize sample preparation and analysis. Our results indicated that sample

thickness, observation depth and laser intensity should all be carefully controlled to avoid the generation of artifacts during image acquisition and facilitate valid comparative studies. We also demonstrated that a simple fixation in 70 % EtOH either before or after section preparation was compatible with the technique thereby facilitating sample collection and processing.

The development of a novel macro in the widely used ImageJ software enabled the generation of a ratiometric image and the subsequent quantification of relevant cell wall lignin levels in selected areas. It should be emphasized that the ratiometric images and derived quantitative data do not represent absolute values such as those obtained by Klason or acetyl bromide analyses (e.g. lignin level expressed as a % of dry cell wall residue). Moreover, since safranin fluorescence can be modulated by a number of different factors (dye concentration, incubation and washing time, sample thickness and observation depth, photobleaching) it is extremely difficult to establish absolute correlation curves. Nevertheless, the technique does provide quantitative values that allow statistically valid comparisons to be made – either between different cell walls/cell wall layers in the same sample, or indeed between cell walls/cell wall layers from different samples (e.g. mutant vs WT plants). This point was demonstrated by our analysis of the previously characterized Arabidopsis *f5h* lignin mutant that has increased lignin content. A comparison of safranin-O ratiometric images and statistical analysis of derived quantitative data indicated statistically significant differences in agreement with previous chemical analysis thereby confirming that the safranin-O method can be used to analyze cell wall lignin levels *in situ* ((Van Acker et al., 2013). Similar analyses of Arabidopsis *cad* and *comt* mutants indicated no statistically significant differences in cell wall lignin levels also in agreement with previous chemical analysis (Van Acker et al., 2013). Although lignin content is unchanged in these two mutants, they do show important modifications in lignin structure (*cad*: increased G units, decreased S units, increased S-unit aldehydes; *comt*: almost total elimination of S units, severely decreased S/G ratio). The fact that these differences did not affect the ratiometric images strongly suggests that the safranin-O based method is insensitive to such changes in lignin structure. As such, it represents a powerful complement to Wiesner staining (sensitive to aldehyde content) and Maüle staining (sensitive to S unit content) for characterizing lignin.

Another important advantage of our method is that it enables quantification for individual cell walls/cell wall layers thereby enabling a much more precise understanding of the effects of mutations on the lignification process in plants. This point was demonstrated by our analysis of the *lac4-2 lac17* double mutant previously characterized by Berthet and co-workers (21). Comparison of ratiometric images from WT and mutant plants enabled us to observe and demonstrate the existence of statistically-significant changes in cell wall lignin levels at both the tissue (xylem vs interfascicular fiber) and cell (vessels vs xylem fiber) levels. Somewhat intriguingly, these analyses also suggested that vessel lignin levels were higher in mutants compared to WT plants.

CONCLUSION

The rapidly increasing availability of relatively low-cost and powerful confocal microscopes is providing scientists with the possibility to revisit old histochemical methods and to develop more efficient, safer, faster and more reproducible approaches, with a better spatial resolution. In this paper we have presented the combination of safranin-O staining coupled to confocal microscopy and an automated image treatment with the free software ImageJ that allows researchers to obtain quantitative data on cell wall lignin content very precisely and to undertake statistically valid comparisons between different cells, either within the same section or between different samples. The toolbox (method plus provided Image J macro) we describe in this paper will create a field of opportunities for modern histology in lignin imaging. It can be used to improve and complete the existing classical staining procedures and other approaches and will contribute to a better understanding of how lignification is regulated at the cellular level.

EXPERIMENTAL PROCEDURES

Plant material and growth conditions

For this study, 4 model plants were used: *Arabidopsis thaliana*, *Linum usitatissimum* (flax), *Populus tremula x P. alba* (poplar) and *Zea mays* (maize). For *Arabidopsis thaliana*, wild-type (Col-0, N60000), and selected 'lignin' mutant lines (*comt1*, *cad6*, *f5h1* (Vanholme et al., 2012) and *lac4-2 lac17* double mutant) were used (Berthet et al., 2011). For *L. usitatissimum*, the Diane fiber variety (WT and *lbf1* mutant) was used (Chantreau et al., 2014). For *P. tremula* x *alba*, the 717-1B4 WT line (INRA clone), was used. For *Z. mays*, an indeterminate forage genotype was used. *A. thaliana*, *L. usitatissimum* and *Z. mays* were grown in soil using a 16h/8h photoperiod, 23°C/20°C temperature, 35-65% hygrometry in a greenhouse with natural light completed with sodium to maintain light intensity at 100 µmol.m^{-2}.s^{-1}. *A. thaliana* plants were harvested at stage 6. *Populus* plants were grown in soil for 2.5 months (60 cm high) in a phytotron with a 16h/8h photoperiod, 24°C/21°C temperature, 35-65% hygrometry with white light (HPI Master Plus Philips, metal halid) to maintain light intensity at 120 µmol.m^{-2}.s^{-1}.

Instruments

Plant stem cross-sections - 80 µm - were made using Microm HV640 and Leica S100 vibroslicers. All the image acquisitions were performed on a LSM710 Confocal (Zeiss) equipped with Argon laser and 541 nm laser and a Nikon A1R confocal equipped with Argon laser and 561 nm laser.

Image J - Fiji macro step development

An Image J - Fiji macro was developed by successive automated steps with possible user intervention at a key point. The steps of the process are as follows : // split channels; // selection of region of interest and subtraction of background noise; // 32 bit conversion and apply median filter radius 1; // set the green image that has the highest intensity value; // apply a threshold and convert the background to NaN; // wait for user to define threshold; // calculate the ratio (plugin ratioplus) ; // copy aaa_lut_fret.lut in the lut field of the Fiji install and run; // Set ratio range; // Measures.

Macro downloading address: https://nextcloud.univ-lille.fr/index.php/s/rKDBBEM3fznRa6Z

Method resume

The complete method is described in the supplementary file Methods S1. A resume scheme of the method is presented in the supplementary figure S1.

ACKNOWLEDGEMENTS

We thank the TisBio facilities and the FRABio research federation for providing the technical environment conducive to achieving this work. We thank Fabienne Guillon for her critical reading of the manuscript. This study was funded by grants from the French Region Hauts de France and the EU (CPER/FEDER project ALIBIOTECH) to F.B.-C. and by the Fonds de la Recherche Scientifique (FRS-FNRS) research project T.0004.14 to F.B.-C and M.B. We thank Prof. Wout Boerjan for providing the *A.thaliana* lines used in this study. We sincerely thank all those who believed in this project, trusted us and supported us in our approach. Thanks to Dr. Nathalie Bessodes without whom this project could not have been possible. I dedicate this work to my daughters Laura and Rosalie.

SUPPORTING INFORMATION LEGENDS

Figure S1. Presentation of the detailed safranin-based fluorescence method.

Figure S2. Illustration of differential settings for the ratiometric representation depending on the chosen color range without affecting ratiometric data for quantification. a) Color range from 0 to 6. b) Color range from 0 to 3. c) Color range from 0 to 1. Scale bar = 150µm.

REFERENCES

AGARWAL, U. P. 2006. Raman imaging to investigate ultrastructure and composition of plant cell walls: distribution of lignin and cellulose in black spruce wood (Picea mariana). *Planta,* 224**,** 1141-53.

AGARWAL, U. P. & RALPH, S. A. 1997. FT-Raman Spectroscopy of Wood: Identifying Contributions of Lignin and Carbohydrate Polymers in the Spectrum of Black Spruce (Picea mariana). *Applied Spectroscopy,* 51**,** 1648-1655.

BASTIN, J. F., FINEGOLD, Y., GARCIA, C., MOLLICONE, D., REZENDE, M., ROUTH, D., ZOHNER, C. M. & CROWTHER, T. W. 2019. The global tree restoration potential. *Science,* 365**,** 76-79.

BERTHET, S., DEMONT-CAULET, N., POLLET, B., BIDZINSKI, P., CEZARD, L., LE BRIS, P., BORREGA, N., HERVE, J., BLONDET, E., BALZERGUE, S., LAPIERRE, C. & JOUANIN, L. 2011. Disruption of LACCASE4 and 17 results in tissue-specific alterations to lignification of Arabidopsis thaliana stems. *Plant Cell,* 23**,** 1124-37.

BOERJAN, W., RALPH, J. & BAUCHER, M. 2003. Lignin biosynthesis. *Annu Rev Plant Biol,* 54**,** 519-46.

BOND, J., DONALDSON, L., HILL, S. & HITCHCOCK, K. 2008. Safranine fluorescent staining of wood cell walls. *Biotech Histochem,* 83**,** 161-71.

CARPITA, N. C. & GIBEAUT, D. M. 1993. Structural models of primary cell walls in flowering plants: consistency of molecular structure with the physical properties of the walls during growth. *Plant J,* 3**,** 1-30.

CHANTREAU, M., PORTELETTE, A., DAUWE, R., KIYOTO, S., CRONIER, D., MORREEL, K., ARRIBAT, S., NEUTELINGS, G., CHABI, M., BOERJAN, W., YOSHINAGA, A., MESNARD, F., GREC, S., CHABBERT, B. & HAWKINS, S. 2014. Ectopic lignification in the flax lignified bast fiber1 mutant stem is associated with tissue-specific modifications in gene expression and cell wall composition. *Plant Cell,* 26**,** 4462-82.

DAY, A., RUEL, K., NEUTELINGS, G., CRONIER, D., DAVID, H., HAWKINS, S. & CHABBERT, B. 2005. Lignification in the flax stem: evidence for an unusual lignin in bast fibers. *Planta,* 222**,** 234-45.

DHARMAWARDHANA, D. P., ELLIS, B. E. & CARLSON, J. E. 1992. Characterization of vascular lignification in Arabidopsis-Thaliana. *Canadian Journal of Botany,* 70**,** 2238-2244.

FROMM, J., ROCKEL, B., LAUTNER, S., WINDEISEN, E. & WANNER, G. 2003. Lignin distribution in wood cell walls determined by TEM and backscattered SEM techniques. *J Struct Biol,* 143**,** 77-84.

FUKUSHIMA, R. S., KERLEY, M. S., RAMOS, M. H., PORTER, J. H. & KALLENBACH, R. L. 2015. Comparison of acetyl bromide lignin with acid detergent lignin and Klason lignin and correlation with in vitro forage degradability. *Animal Feed Science and Technology,* 201**,** 25-37.

GIERLINGER, N. 2014. Revealing changes in molecular composition of plant cell walls on the micron-level by Raman mapping and vertex component analysis (VCA). *Front Plant Sci,* 5**,** 306.

GIERLINGER, N. 2018. New insights into plant cell walls by vibrational microspectroscopy. *Appl Spectrosc Rev.*

HOSMANI, P. S., KAMIYA, T., DANKU, J., NASEER, S., GELDNER, N., GUERINOT, M. L. & SALT, D. E. 2013. Dirigent domain-containing protein is part of the machinery required for formation of the lignin-based Casparian strip in the root. *Proc Natl Acad Sci U S A,* 110**,** 14498-503.

JOHNSON, D. B., MOORE, W. E. & ZANK, L. C. 1961. The spectrophotometric determination of lignin in small wood samples. *TAPPI journal,* 44**,** 793-798.

KIYOTO, S., YOSHINAGA, A., TANAKA, N., WADA, M., KAMITAKAHARA, H. & TAKABE, K. 2013. Immunolocalization of 8-5' and 8-8' linked structures of lignin in cell walls of Chamaecyparis obtusa using monoclonal antibodies. *Planta,* 237**,** 705-15.

LAPIERRE, C., MONTIES, B. & ROLANDO, C. 1986. Thioacidolysis of Poplar Lignins: Identification of Monomeric Syringyl Products and Characterization of Guaiacyl-Syringyl

Lignin Fractions. *Holzforschung - International Journal of the Biology, Chemistry, Physics and Technology of Wood.*

LEGLAND, D., EL-HAGE, F., MECHIN, V. & REYMOND, M. 2017. Histological quantification of maize stem sections from FASGA-stained images. *Plant Methods,* 13**,** 84.

LILJEGREN, S. 2010. Phloroglucinol stain for lignin. *Cold Spring Harb Protoc,* 2010**,** pdb prot4954.

MANSFIELD, S. D., KIM, H., LU, F. & RALPH, J. 2012. Whole plant cell wall characterization using solution-state 2D NMR. *Nat Protoc,* 7**,** 1579-89.

MESHITSUKA, G. & NAKANO, J. 1979. Studies on the mechanism of lignin color reaction. XIII. Maule color reaction. *J. Japanese Wood Res. Soc.,* 25**,** 588-594.

MONTIES, B. 1989. Lignins. *In:* DEY, P. M. & HARBORNE, J. B. (eds.) *Methods in plant biochemistry.* London ; San Diego: Academic Press.

MORRISON, I. M. 1972a. Improvements in the acetyl bromide technique to determine lignin and digestibility and its application to legumes. *Journal of the Science of Food and Agriculture,* 23**,** 1463-1469.

MORRISON, I. M. 1972b. A semi-micro method for the determination of lignin and its use in predicting the digestibility of forage crops. *journal of the Science of Food and Agriculture,* 23**,** 455-463.

PESQUET, E., RANOCHA, P., LEGAY, S., DIGONNET, C., BARBIER, O., PICHON, M. & GOFFNER, D. 2005. Novel markers of xylogenesis in zinnia are differentially regulated by auxin and cytokinin. *Plant Physiol,* 139**,** 1821-39.

SIMON, C., LION, C., BIOT, C., GIERLINGER, N. & HAWKINS, S. 2018. Lignification and Advances in Lignin Imaging in Plant Cell Walls. *Annual Plant Reviews,* 1**,** 1-32.

STOCKERT, J. C., CANETE, M. & COLMAN, O. D. 1984. Histochemical mechanism for the orthochromatic staining and fluorescence reaction of lignified tissues. *Cell Mol Biol,* 30**,** 503-8.

TERASHIMA, N. & FUKUSHIMA, K. 1988. Heterogeneity in formation of lignin—XI: An autoradiographic study of the heterogeneous formation and structure of pine lignin. *Wood Science and Technology,* 22**,** 259-270.

TOBIMATSU, Y. & SCHUETZ, M. 2019. Lignin polymerization: how do plants manage the chemistry so well? *Curr Opin Biotechnol,* 56**,** 75-81.

TOLIVIA, D. & TOLIVIA, J. 1987. Fasga: A New Polychromatic Method for Simultaneous and Differential Staining of Plant Tissues. *Journal of Microscopy (Oxford),* 148**,** 113-117.

VALLET, C., CHABBERT, B., CZANINSKI, Y. & MONTIES, B. 1996. Histochemistry of Lignin Deposition during Sclerenchyma Differentiation in Alfalfa Stems. *Annals of Botany,* 78**,** 625-632.

VAN ACKER, R., VANHOLME, R., STORME, V., MORTIMER, J. C., DUPREE, P. & BOERJAN, W. 2013. Lignin biosynthesis perturbations affect secondary cell wall composition and saccharification yield in Arabidopsis thaliana. *Biotechnol Biofuels,* 6**,** 46.

VAN SOEST, P. J. 1963. Use of detergents in the analysis of fibrous foods. II. A rapid method for the determination of fibre and lignin. *Journal - Association of Official Analytical Chemists,* 46**,** 829-835.

VANHOLME, R., STORME, V., VANHOLME, B., SUNDIN, L., CHRISTENSEN, J. H., GOEMINNE, G., HALPIN, C., ROHDE, A., MORREEL, K. & BOERJAN, W. 2012. A Systems Biology View of Responses to Lignin Biosynthesis Perturbations in Arabidopsis[W]. *Plant Cell,* 24**,** 3506-29.

WAGNER, A., RALPH, J., AKIYAMA, T., FLINT, H., PHILLIPS, L., TORR, K., NANAYAKKARA, B. & TE KIRI, L. 2007. Exploring lignification in conifers by silencing hydroxycinnamoyl-CoA:shikimate hydroxycinnamoyltransferase in Pinus radiata. *Proc Natl Acad Sci U S A,* 104**,** 11856-61.

YI CHOU, E., SCHUETZ, M., HOFFMANN, N., WATANABE, Y., SIBOUT, R. & SAMUELS, A. L. 2018. Distribution, mobility, and anchoring of lignin-related oxidative enzymes in Arabidopsis secondary cell walls. *J Exp Bot,* 69**,** 1849-1859.

FIGURE LEGENDS

Figure 1. Cell wall associated safranin spectra. a) Flax stem cross-section stained with toluidine blue showing tissue organization and region of interest (yellow dotted circles) used for safranin spectra acquisition, b) Safranin spectra (excitation 488nm) of 4 regions of interest from cells known to contain different amounts of lignin: “low”, (bast fiber cell wall, spectra 1, orange line; cambial cell wall, spectra 2, blue line), “high” (xylem cell walls, spectra 3 and 4, green and yellow lines). bf = bast fibers, c = cortex, cz = cambial zone, m = medulla, p = phloem, px = primary xylem, x = xylem. Scale bar = 100µm

Figure 2. Presentation of safranin-based fluorescence method. a) Acquisition of the green part of the safranin spectra (ex:488nm, em:540-560nm), b) Acquisition of the red part of the safranin spectra (ex:561nm, em:570-600nm), c) ratiometric image resulting from red and green image treatment using the Image J macro developed, d) Ratio quantification in different parts of the section. The Region Of Interest (ROI) 1 corresponds to the safranin ratio from hypolignified flax fibers. The ROI 2 corresponds to the safranin ratio from lignified flax xylem. The range color used for image representation goes from ratio 0 (purple) to ratio 2 (red). bf = bast fibers, c = cortex, cz = cambial zone, x = xylem. Scale bar = 100µm

Figure 3. Biological validation of the method in Arabidopsis monolignol biosynthetic pathway mutants. From a) to c) are represented safranin ratiometric images of interfascicular fibers from floral stem cross sections of Col-0 line (a), *comt* mutant (b) and *f5h* mutant (c) from a first experiment. In d) and e) are respectively represented safranin ratiometric images of interfascicular fibers from floral stem cross sections of Col-0 line (a), cad mutant (e) from a second independent experiment. f) Histograms of average safranin ratios for each analyzed line, values show no significant differences except * = significant difference at $P<0.01$. The color range used for the image representations goes from ratio 0 (purple) to ratio 1.5 (red). Scale bar = 50µm.

Figure 4. Biological validation of the method in Arabidopsis *lac4-2 lac17* mutant. From a) to b) are represented safranin ratiometric images of interfascicular fibers from floral stem cross sections of Col-0 line (a) and *lac4-2 lac17* mutant (b). c) Histograms of average and maximum safranin ratios. From d)

to e) are represented safranin ratiometric images of xylem bundle from floral stem cross sections of Col-0 line (d) and *lac4-2 lac17* mutant (e). f) Histogram of xylem bundle average safranin ratios. f) Histogram of xylem vessels average safranin ratios. * = significant difference at P=0.01. The color range used for the image representations goes from ratio 0 (purple) to ratio 2 (red). Scale bar = 50µm.

Figure 5. Biological validation of the method in other plant species: flax. From a) to c) are represented safranin ratiometric images of flax stem cross sections of WT (a) and LBF1 mutant of 4weeks old (b and c) plants. The color range used for the image representations varies from ratio 0 (purple) to ratio 2 (red). d) histogram of average safranin ratio and e) histogram of maximum safranin ratio for each analyzed line. bf = bast fibers, c = cortex, cz = cambial zone, x = xylem. Scale bar = 50µm

Figure 6. Biological validation of the method in other plant species: maize. a) Safranin ratiometric image of a stem cross-section of maize observed with a 4x objective. b) Safranin ratiometric image of a vascular bundle from a stem cross-section of maize observed with a 60x objective. c) Histograms of average intensity safranin ratios for epidermis, hypodermis and external vascular bundles. The range color used for image representation varies from ratio 0 (purple) to ratio 1.5 (red). bs = bundle sclerenchyma, e = epidermis, mx = metaxylem, pa = parenchyma, ph = phloem, px = protoxylem, vb = vascular bundle. Scale bar a) = 1mm and b) = 100µm.

Figure 7. Flax xylem cell walls: the finesse of the method. a) Safranin ratiometric images of xylem cross sections from 8-weeks-old flax stems observed with a 60x objective. b) Detail of a pit and anticlinal walls from a). Arrows show periclinal xylem cell walls. Scale bar = 15µm

Figure 8. Effect of depth and flatness on the safranin ratio. (a) Analysis of green and red channel fluorescence intensity in several Z-optical sections of poplar xylem. Graphical representation of the fluorescence intensity of both channels for 15 optical sections of 6.15µm. Green line corresponds to green channel. Red line corresponds to red channel. Grey area corresponds to the optimal section for analysis and comparison of several independent plant sections. (b) Analysis of *A. thaliana* floral stem cross section. From i) to iv) images of cell wall lignin in a vascular bundle obtained at 4 different optical

focal planes. For each optical section, a synthetic sketch illustrates the corresponding image along the A-B section in term of color corresponding to safranin ratio depending on the depth. Scale bar = 50µm.

Figure 9. Effects of laser energy (intensity and time) on cell wall images and green/red ratio. The effects of different 488nm excitation energies were evaluated on fiber poplar cross sections stained with safranin O. From a) to c) analysis of safranin ratiometric image with a low excitation power (5%). From d) to f) analysis of safranin ratiometric image with a high excitation power (100%). a) and d) correspond to one optimal pass acquisition, b) and e) correspond to the image after the 7th pass and c) and f) correspond to the image at the 15th pass. g) Quantitative analysis of red/green safranin ratios for 15 pass acquisitions. White bars correspond to safranin ratio evolution at low laser intensity and black bars correspond to safranin ratio evolution at high laser intensity. The 1st pass acquisition is normalized to 100% for both laser conditions. h) Safranin ratiometric image of poplar fibers including an insert delimited by a dotted line representing the safranin ratiometric fibers after 15 pass acquisitions.

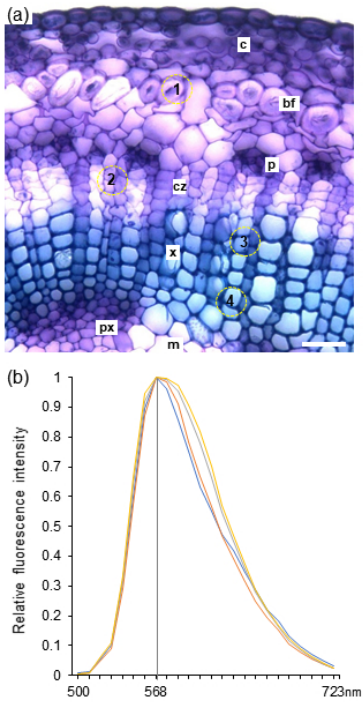

Figure 1.

Cell wall associated safranin spectra. a) Flax stem cross-section stained with toluidine blue showing tissue organization and region of interest (yellow dotted circles) used for safranin spectra acquisition, b) Safranin spectra (excitation 488nm) of 4 regions of interest from cells known to contain different amounts of lignin: "low", (bast fiber cell wall, spectra 1, orange line; cambial cell wall, spectra 2, blue line), "high" (xylem cell walls, spectra 3 and 4, green and yellow lines). bf = bast fibers, c = cortex, cz = cambial zone, m = medulla, p = phloem, px = primary xylem, x = xylem. Scale bar = 100µm

190x275mm (96 x 96 DPI)

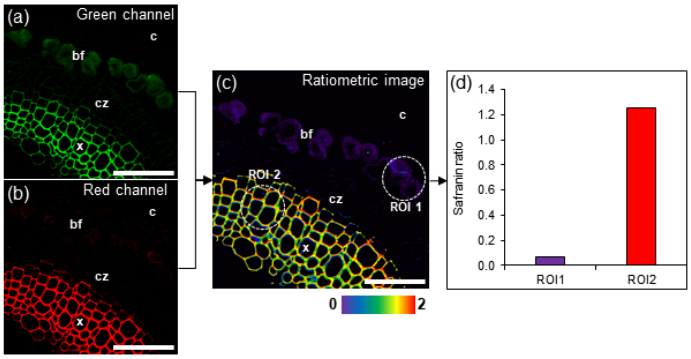

Figure 2.

Presentation of safranin-based fluorescence method. a) Acquisition of the green part of the safranin spectra (ex:488nm, em:540-560nm), b) Acquisition of the red part of the safranin spectra (ex:561nm, em:570-600nm), c) ratiometric image resulting from red and green image treatment using the Image J macro developed, d) Ratio quantification in different parts of the section. The Region Of Interest (ROI) 1 corresponds to the safranin ratio from hypolignified flax fibers. The ROI 2 corresponds to the safranin ratio from lignified flax xylem. The range color used for image representation goes from ratio 0 (purple) to ratio 2 (red). bf = bast fibers, c = cortex, cz = cambial zone, x = xylem. Scale bar = 100µm

190x275mm (96 x 96 DPI)

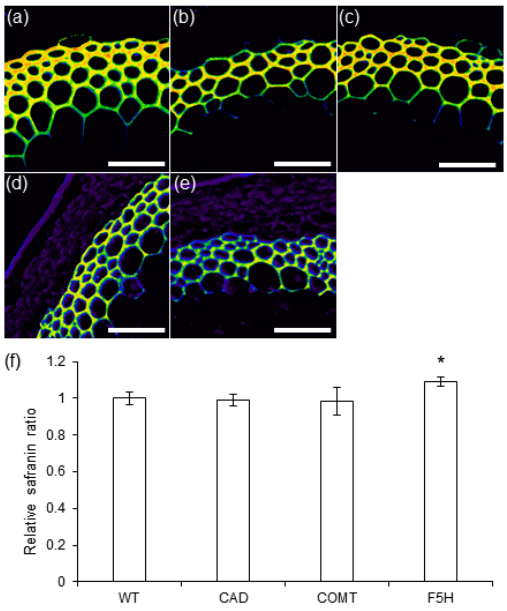

Figure 3.

Biological validation of the method in Arabidopsis monolignol biosynthetic pathway mutants. From a) to c) are represented safranin ratiometric images of interfascicular fibers from floral stem cross sections of Col-0 line (a), comt mutant (b) and f5h mutant (c) from a first experiment. In d) and e) are respectively represented safranin ratiometric images of interfascicular fibers from floral stem cross sections of Col-0 line (a), cad mutant (e) from a second independent experiment. f) Histograms of average safranin ratios for each analyzed line, values show no significant differences except * = significant difference at $P<0.01$. The color range used for the image representations goes from ratio 0 (purple) to ratio 1.5 (red). Scale bar = 50µm.

190x275mm (96 x 96 DPI)

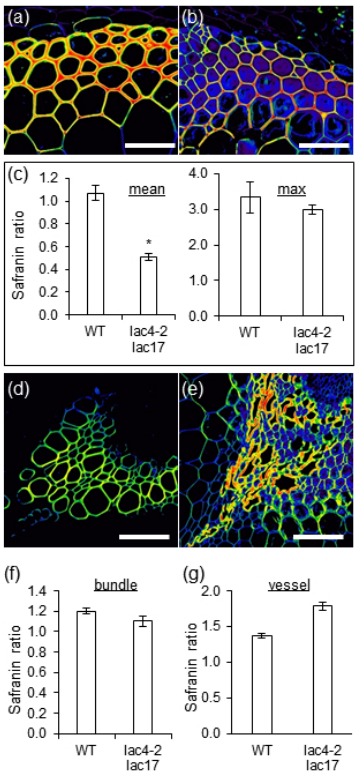

Figure 4.

Biological validation of the method in Arabidopsis lac4-2 lac17 mutant. From a) to b) are represented safranin ratiometric images of interfascicular fibers from floral stem cross sections of Col-0 line (a) and lac4-2 lac17 mutant (b). c) Histograms of average and maximum safranin ratios. From d) to e) are represented safranin ratiometric images of xylem bundle from floral stem cross sections of Col-0 line (d) and lac4-2 lac17 mutant (e). f) Histogram of xylem bundle average safranin ratios. f) Histogram of xylem vessels average safranin ratios. * = significant difference at P=0.01. The color range used for the image representations goes from ratio 0 (purple) to ratio 2 (red). Scale bar = 50µm.

190x275mm (96 x 96 DPI)

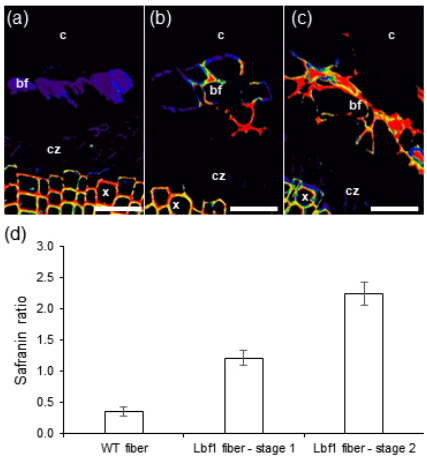

Figure 5.

Biological validation of the method in other plant species: flax. From a) to c) are represented safranin ratiometric images of flax stem cross sections of WT (a) and LBF1 mutant of 4weeks old (b and c) plants. The color range used for the image representations varies from ratio 0 (purple) to ratio 2 (red). d) histogram of average safranin ratio and e) histogram of maximum safranin ratio for each analyzed line. bf = bast fibers, c = cortex, cz = cambial zone, x = xylem. Scale bar = 50µm

190x275mm (96 x 96 DPI)

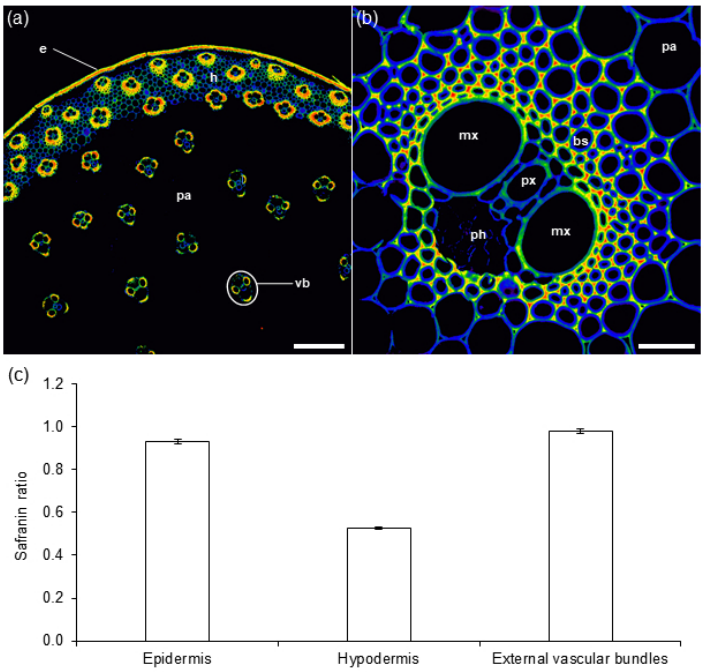

Figure 6.

Biological validation of the method in other plant species: maize. a) Safranin ratiometric image of a stem cross-section of maize observed with a 4x objective. b) Safranin ratiometric image of a vascular bundle from a stem cross-section of maize observed with a 60x objective. c) Histograms of average intensity safranin ratios for epidermis, hypodermis and external vascular bundles. The range color used for image representation varies from ratio 0 (purple) to ratio 1.5 (red). bs = bundle sclerenchyma, e = epidermis, mx = metaxylem, pa = parenchyma, ph = phloem, px = protoxylem, vb = vascular bundle. Scale bar a) = 1mm and b) = 100µm.

190x275mm (96 x 96 DPI)

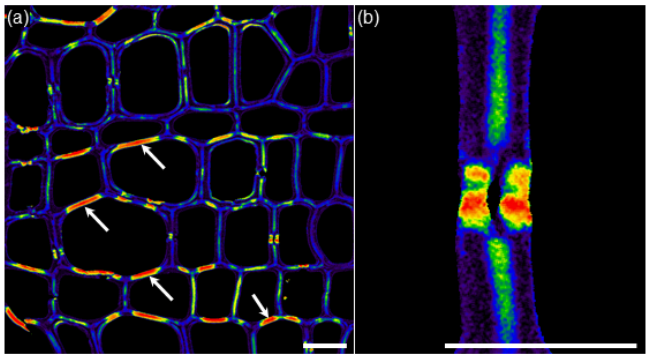

Figure 7.

Flax xylem cell walls: the finesse of the method. a) Safranin ratiometric images of xylem cross sections from 8-weeks-old flax stems observed with a 60x objective. b) Detail of a pit and anticlinal walls from a). Arrows show periclinal xylem cell walls. Scale bar = 15µm

190x275mm (96 x 96 DPI)

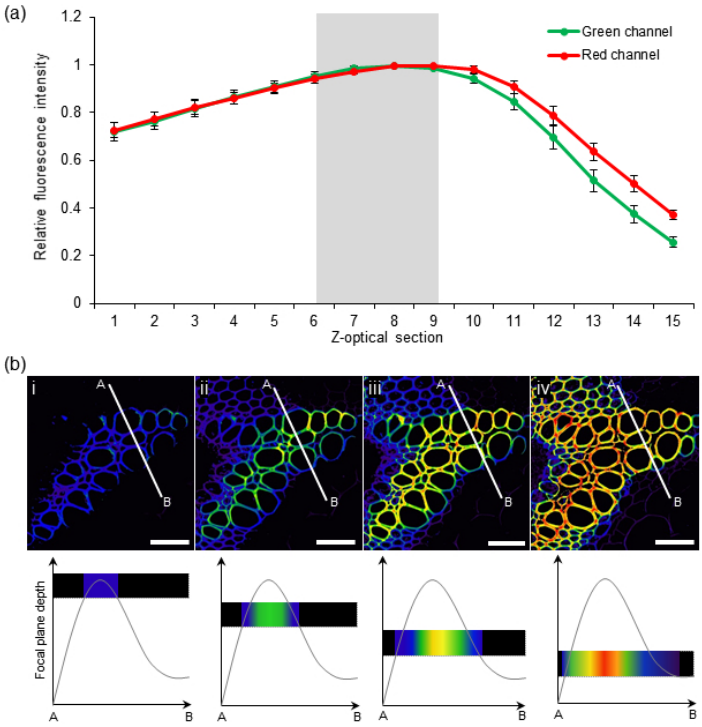

Figure 8.

Effect of depth and flatness on the safranin ratio. (a) Analysis of green and red channel fluorescence intensity in several Z-optical sections of poplar xylem. Graphical representation of the fluorescence intensity of both channels for 15 optical sections of 6.15µm. Green line corresponds to green channel. Red line corresponds to red channel. Grey area corresponds to the optimal section for analysis and comparison of several independent plant sections. (b) Analysis of A. thaliana floral stem cross section. From i) to iv) images of cell wall lignin in a vascular bundle obtained at 4 different optical focal planes. For each optical section, a synthetic sketch illustrates the corresponding image along the A-B section in term of color corresponding to safranin ratio depending on the depth. Scale bar = 50µm.

190x275mm (96 x 96 DPI)

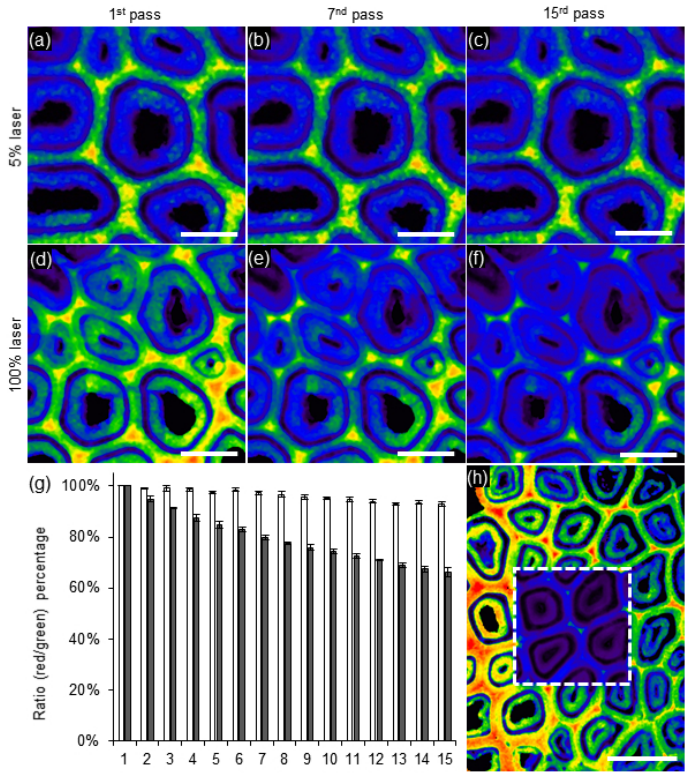

Figure 9.

Effects of laser energy (intensity and time) on cell wall images and green/red ratio. The effects of different 488nm excitation energies were evaluated on fiber poplar cross sections stained with safranin O. From a) to c) analysis of safranin ratiometric image with a low excitation power (5%). From d) to f) analysis of safranin ratiometric image with a high excitation power (100%). a) and d) correspond to one optimal pass acquisition, b) and e) correspond to the image after the 7th pass and c) and f) correspond to the image at the 15th pass. g) Quantitative analysis of red/green safranin ratios for 15 pass acquisitions. White bars correspond to safranin ratio evolution at low laser intensity and black bars correspond to safranin ratio evolution at high laser intensity. The 1st pass acquisition is normalized to 100% for both laser conditions. h) Safranin ratiometric image of poplar fibers including an insert delimited by a dotted line representing the safranin ratiometric fibers after 15 pass acquisitions.

190x275mm (96 x 96 DPI)

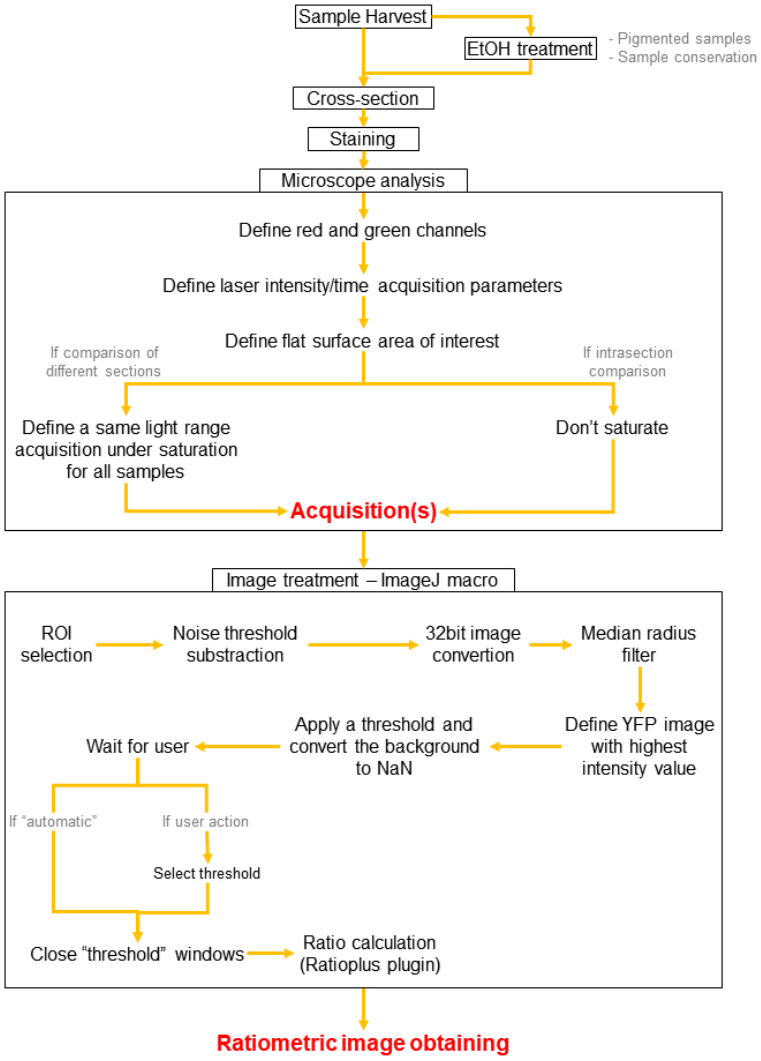

Figure S1.

Presentation of the detailed safranin-based fluorescence method.

190x275mm (96 x 96 DPI)

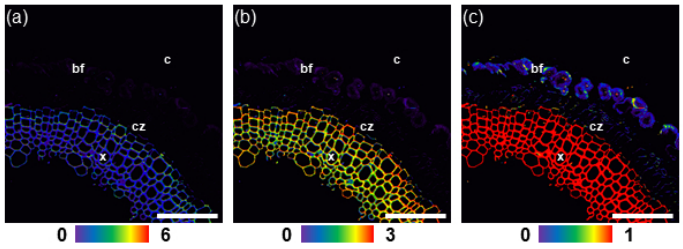

Figure S2.

Illustration of differential settings for the ratiometric representation depending on the chosen color range without affecting ratiometric data for quantification. a) Color range from 0 to 6. b) Color range from 0 to 3. c) Color range from 0 to 1. Scale bar = 150µm.

190x275mm (96 x 96 DPI)

Methods S1

Baldacci-Cresp F., et al.

A rapid and semi-quantitative safranin-based fluorescent microscopy method to evaluate cell wall lignification

CHEMICALS:

The following chemicals were used to develop the protocol: Agarose (Sigma, CAS-No: 30525-89-4), Safranin-O (Sigma, CAS-No: 477-73-6), ethanol (Sigma, CAS-No: 64-17-5) and that's all.

SAFRANIN-O SOLUTION:

- **Ethanol** [final 50% (w/v)],
- **Safranin-O** [final 0.2% (w/v)]
- **Ultrapure water** to the final volume

Mix the solution well for at least 15min until you get everything completely dissolved.

PREPARATION OF THE SOLUTION AND ITS STORAGE

- Safranin-O is purchased as a powder and dissolved in ethanol 50% solution.
- To prepare the staining solutions, weigh the indicated amount of the corresponding dye powder, dissolve it in ethanol 50% solution by mixing the solution on the magnetic stirrer in a small flask for at least 15min.
- To store the solutions, wrap them in aluminium foil to avoid exposing them to light at 4°C.

Note 1: if possible prefer fresh safranin-O solution.

Note 2: for long term conservation, a 10x solution can be prepared, split in aliquots and keep several months in the dark at -20°C.

SAMPLE TREATMENT

- Collect samples, maximum 0.5 cm length.
- Place them in 70% EtOH overnight with shaking at 4°C to fix and remove pigments that can impact the fluorescence acquisition.
- Remove alcohol solution.

- Coat samples in moult with agarose solution (3 to 4%).
- Perform section - ideally from 30µm to 100µm - on a vibroslicer and place them on EtOH 50% solution until staining. For this step and depending on your samples and the vibroslicer you must adapt section parameters (speed, frequency, amplitude section) to obtain the best morphology. Better the samples morphology is kept better will be the results.

  Note: the same procedure can be envisaged with other embedding as paraffin or PEG to use microtome instead of vibroslicer to obtain better morphology. In this case the global procedure will be longer. However, the gain in morphological quality is justified only for fragile tissues.

SAFRANIN-O STAINING

- Prepare fresh 0.2% Safranin-O.
- Place vibrosliced samples in safranine-O solution for 10min under shacking at RT at obscurity.
- Remove all safranine-O solution.
- Rinse one time in ethanol 50% solution for 10min under shacking at RT at obscurity.
- Remove all the solution.
- Rinse two time in ultrapure water for 15min under shacking at RT at obscurity.
- Mount samples in water for imaging.

Note 1: For the staining and for rinsing it's important to have a big volume of solution compared to sample number and to incubate in container allowing good homogenization under shaking.

Note 2: Adapt the flushing time if necessary. Young lignified tissues or tissues with low lignin content don't support too high decolouring time.

Note 3: Never mount your samples in glycerol or glycerol-containing mounting medium because safranin-O is highly soluble in glycerol.

CONFOCAL ANALYSIS

For the first analysis:

- Perform a comparative spectra analysis between lignified and non-lignified tissue. This step is essential to determine the peak of maximum intensity, the invariable area of the spectrum (green part, generally between 520nm and 560 nm) and the area of the spectrum sensitive to lignin quantity (yellow to red part, generally between the maximum intensity peak and 630 nm).
- For the spectral analysis use a 488nm excitation coupled with acquisition from 500nm to 700nm. Warning: limit 488 nm laser power and pixel time exposition to avoid spectra alteration as presented in this study.

Current analysis:

- To optimize results and limiting 488nm laser using to avoid spectral shift, the acquisition was developed with 2 independent track with two different laser line excitation.

  Track 1- green channel - ex: 488nm, em: 530-560 nm – limit 488 nm laser power (1-5% on recent laser).

  Track 2- red channel - ex: 561nm, em: 570-600 nm.
- Considering the semi-quantitative comparison between independent samples, settings of the reference sample must limit light range acquisition to 70% of the maximum tones (about 2900 tones for 12 bit image acquisition).
- Acquire sequentially both tracks.

Note: Acquisition parameters depend on the confocal microscope used. The important point is to well define the green and the red channel and adapt the parameters in function of.

IMAGE TREATMENT

- For the image treatment use the Fiji install completed with the developed macro available to this address: (https://nextcloud.univ-lille.fr/index.php/s/rKDBBEM3fznRa6Z).
- Open the Fiji app
- Open the macro file with Fiji.
- Open the image.
- Run the macro and follow the instructions.

  The result is a ratiometric image (representing ratio range from 0 to 2).

Note 1: if the macro is completely automated, the user has the possibility to act on the threshold applied to image treatment. Let the automatic threshold choice except if you consider that the morphology doesn't correspond to your scientific knowledge of the model studied.

Note 2: Two parameters of the macro can be adjusted depending on the acquisition.

- The "rooling" must be adapted according to image resolution and size of the analysed biological structure which vary with the objective used and the zoom used for the acquisition.
- The ratio range representation is set from 0 to 2 (purple to red). If the variation is more or less important, the ratiometric range can be adjusted to optimize representation. In this case, the same range must be applied to all image included in the comparison. Modify the range don't modify raw pixel values.